*32nd EPS Conference on Plasma Phys. Tarragona, 27 June - 1 July 2005 ECA Vol.**29C**, P-1.042 (2005)*

Transient electron heat transport and reduced density fluctuation after pellet injection in JT-60U reversed shear plasmas

H. Takenaga[1], N. Oyama[1], A. Isayama[1], S. Inagaki[2], T. Takizuka[1], T. Fujita[1], Y. Miura[1]

[1] *Naka Fusion Research Establishment, Japan Atomic Energy Research Institute, 801-1 Mukouyama, Naka, Ibaraki 311-0193, Japan*

[2] *National Institute for Fusion Science, 322-6 Oroshi-cho, Toki, Gifu 509-5292, Japan*

1. Introduction

Understanding of anomalous turbulent transport is a crucial issue, especially for electron heat transport, because it remains at an anomalous level even with the ion heat transport reduced to the neoclassical level. The electron thermal diffusivity decreases to the same level as the ion neoclassical heat diffusivity, but still higher than the electron neoclassical heat diffusivity in the strong internal transport barrier (ITB). In order to understand the mechanism for the suppression of the anomalous turbulent transport in the ITB region, density fluctuation has been measured. In a TFTR enhanced reversed shear (RS) mode, the reduction of the density fluctuation level and the ITB formation were observed at the same time when the E×B shearing rate exceeded the linear growth rate [1]. In the ITB formation phase of JT-60U RS plasmas, the reduction of the correlation length for the density fluctuation was observed, although the reduction of its level was not observed [2]. In contrast, drastic reduction of the density fluctuation level was measured in the ITB region, when a pellet was injected into a JT-60U RS plasma with the strong ITB [3]. In this paper, transient electron heat transport is investigated in relation to the reduction of the density fluctuation level after the pellet injection for understanding the mechanism regulating the electron heat transport.

2. Reduction of density fluctuation level after the pellet injection

Figure 1 shows wave-forms in a RS plasma, where the reduction of density fluctuation level was observed after the pellet injection. The plasma current I_p=2.2 MA and the toroidal magnetic field B_T=4.3 T were adopted in an inward shifted configuration. The first pellet was injected at t=6.32 s from high-field-side at the top [4] after the strong ITB formation, as shown by the edge density jump, during the I_p flat-top phase with the constant heating power of neutral beam (NB). The edge density profile measured just after the pellet injection indicated that the pellet reached to the position of r/a~0.8. After the first pellet injection, the central density and the stored energy started to increase. A high frequency component (|f|>200 kHz) of the O-mode reflectometer signal was drastically reduced, as well as the low frequency component (|f|<50 kHz), ~5 ms after the pellet injection. The cut-off layer (at n_e=2.8×10^{19} m^{-3})

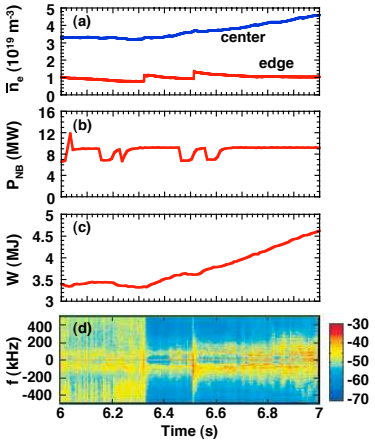

Fig. 1 Wave-forms of a RS plasma, where density fluctuation was reduced after the pellet injection. (a) Center and edge line averaged electron densities, (b) neutral beam heating power, (c) stored energy and (d) spectrogram of the O-mode reflectometer signal.

was located in the ITB region. The density fluctuation level $\tilde{n}/n$ was estimated from the O-mode reflectometer signal based on the analytical solution of time-dependent 2D full-wave equation [5]. The value of $\tilde{n}/n$ was estimated to be 1-2% before and 0.4-0.6% after the first pellet injection, respectively [3].

The profiles of density, temperature, effective particle diffusivity and thermal diffusivity are shown in Fig. 2 before (t=6.3 s) and after (t=7.0 s) the pellet injections. The density profile inside the ITB foot was not measured in this configuration. Therefore, it was evaluated based on the interferometer signal for the central chord and the carbon density profile measured with charge exchange recombination spectroscopy. It is noted that the shape of the carbon density profile is similar to the shape of the electron density profile in RS ITB plasmas with other configurations on JT-60U [6]. The density substantially increased inside the ITB, while the edge density slightly increased. The cut-off layer of the O-mode reflectometer is located around r/a~0.45 at t=6.3 s and r/a~0.5 at t=7.0 s, respectively. The ion and electron temperature (T_i and T_e) profiles were not largely changed as shown in Fig. 2 (b). The strong T_i ITB and the moderate T_e ITB were maintained with the ITB foot position around r/a=0.6.

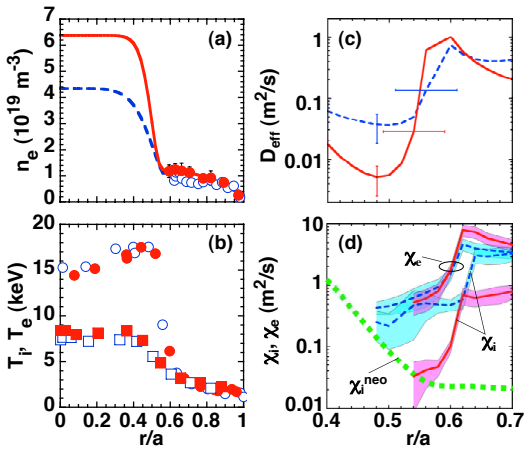

Fig. 2 Profiles of (a) density, (b) temperature, (c) effective particle diffusivity and (d) electron and ion thermal diffusivities, before (t=6.3 s : open symbols and/or dashed lines) and after (t=7.0 s : closed symbols and/or solid lines) the pellet injections. In (b), circles and squares indicate the ion and electron temperatures, respectively. The neoclassical ion thermal diffusivity is also shown by a dotted line in (d).

The effective particle diffusivity and the thermal diffusivity were estimated by the particle and power balance analysis without consideration of the pinch term. The effective particle diffusivity and the ion thermal diffusivity (χ_i) decreased remarkably after the pellet injections, as shown in Fig. 2 (c) and (d). The equi-partition heat transfer from ions to electrons increased due to the substantial increase in the central density, but no change of difference between T_i and T_e was observed. The T_i gradient in the ITB region was maintained with the decreased ion heat flux after the pellet injections due to χ_i reduced to a neoclassical level. On the contrary, no reduction of the electron thermal diffusivity (χ_e) was observed. The increase in the electron stored energy (density increase with a constant T_e) was attributed to the increase in the equi-partition heat transfer from ions.

3. Transient electron heat transport

Transient response of the electron heat transport during the $\tilde{n}/n$ reduction was investigated. Time evolution of T_e measured from electron cyclotron emission is shown in Fig. 3 together with time evolution of the integrated power for high frequency component (|f|>200 kHz) of the O-mode reflectometer signal ($P_{refl.}^{H}$). The value of $P_{refl.}^{H}$ was estimated using Fourier transform in the time window of every 5 ms. The edge T_e at r/a~0.85 was sharply dropped by the ablation of pellet cloud. The cold pulse induced by the pellet ablation propagated from the outside of the ITB into the strong ITB region. When the cold pulse

propagated to the position of r/a=0.54 in the strong ITB region at t=6.325 s, $P_{refl.}^{H}$ was drastically reduced with a short time scale (<5 ms). At this timing, T_e outside the ITB (r/a=0.6-0.85) was decreased by the cold pulse propagation, while T_e in the ITB region (r/a<0.54) was not changed, as shown in Fig. 3 (c), due to slower propagation speed of the cold pulse in the ITB region. Thus, T_e gradient became large in the outer ITB portion at t=6.325 s. The value of T_e at r/a=0.54 largely decreased after the $P_{refl.}^{H}$ reduction, and the ITB structure seems to be destroyed in the outer ITB portion (r/a=0.54-0.64) at t=6.35 s, as shown in Fig. 3 (c). The reduction of T_e was larger at r/a=0.54 than outside the ITB. The larger T_e reduction in the ITB region during the cold pulse propagation was also observed in JT-60U RS (without the $\tilde{n}/n$ reduction), JET optimized shear and LHD electron ITB plasmas [7, 8]. It seems to be common phenomena in toroidal plasmas even without the $\tilde{n}/n$ reduction. The cold pulse propagation was stopped in the inner ITB portion and T_e around the ITB shoulder did not decrease. Therefore, the T_e gradient became large in the inner ITB portion at t=6.35 s. After t=6.35 s, T_e at r/a=0.54 started to increase. Finally, the T_e profile was recovered with a time constant of about 200 ms.

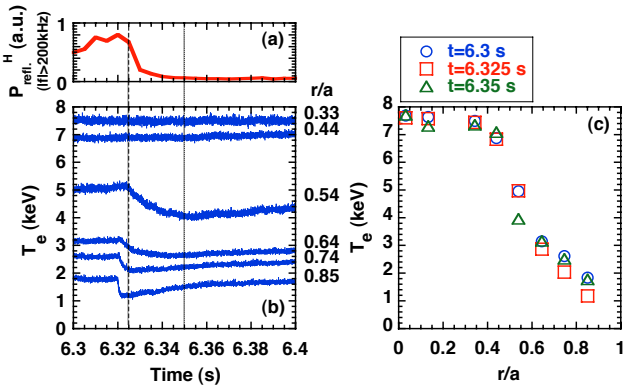

Fig. 3 (a) Time behavior of the integrated power of high frequency component (|f|>200 kHz) of the O-mode reflectometer signal. (b) Time evolution of the electron temperature. (c) Circles, squares and triangles show the electron temperature profile before the pellet injection, at the timing for reduction of density fluctuation (dashed line in (a)) and at the timing for maximum electron temperature reduction at r/a=0.54 (dotted line in (a)), respectively.

The transient T_e response was simulated using models on χ_e described below until 20 ms after the pellet injection (until t=6.34 s). In the simulation, the profiles of the electron heating power deposition including the equi-partition heat transfer and the particle source estimated from the power and particle balance analysis before the pellet injection (t=6.3 s) were used. The power balance analysis indicated the importance of equi-partition heat transfer. Since the change of electron heating power due to the change in T_e was small in the simulated duration (20 ms), the change of the equi-patition heat transfer power was not considered in this simulation. First, the transient time behavior was simulated with the χ_e profile estimated from the power balance at t=6.3 s. The reduction of the calculated T_e was remarkably smaller than the measured one at r/a=0.54 in the ITB region. The power balance χ_e did not reproduce the measured T_e time evolution in the ITB region.

Next, time evolution of χ_e was adjusted in order to reproduce the T_e time behavior. In this case, strong T_e dependence of χ_e was assumed as $\chi_e \propto T_e^{-2.3}$ in the outer ITB portion (r/a=0.54-0.62) to reproduce the larger T_e reduction at r/a=0.54. The transient cold pulse analysis in JT-60U RS ITB plasmas without the $\tilde{n}/n$ reduction and LHD electron ITB plasmas has shown the existence of such strong negative T_e dependence of χ_e [7]. The larger T_e reduction at r/a=0.54 leads to the increase in the heat flux to the outside of the ITB and the increase in the electron temperature gradient (∇T_e) in the inner ITB portion compared with

the power balance χ_e case. Weak negative T_e dependence of χ_e was assumed as $\chi_e \propto T_e^{-0.5}$ outside the ITB (r/a>0.63) to reproduce the measurement with the increased heat flux outside the ITB. Furthermore, in the inner ITB portion (r/a=0.3-0.5), it was assumed that χ_e is inversely proportional to ∇T_e as $\chi_e \propto \nabla T_e^{-1}$ for keeping the electron heat flux constant against the increase in ∇T_e. In this case, the value of χ_e decreased in the inner ITB portion and increased in the outer ITB portion depending on the T_e profile change, as shown in Fig. 4 (a). At Δt=+20 ms, χ_e decreased by a factor of 2 in the inner ITB portion (near the cut-off layer of the O-mode reflectometer) and increased by a factor of 1.5 in the outer ITB portion. The time behavior of the calculated T_e well agreed with the measurement, as shown in Fig. 4 (b).

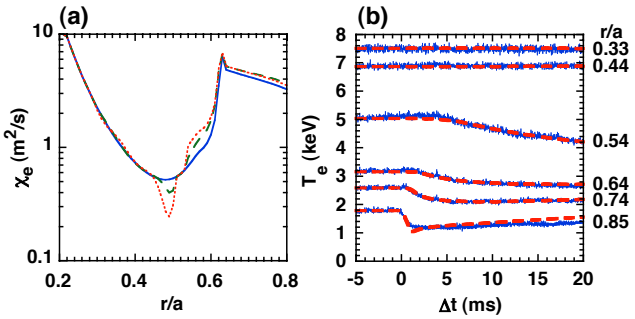

Fig. 4 (a) The χ_e profiles used for the simulation. Solid, dashed and dotted lines indicate the χ_e profiles before the pellet injection, at Δt=+10 ms and +20 ms, respectively. (b) Comparison of time behavior of the electron temperature between simulation (dashed line) and measurement (solid line).

4. Discussions

The simulation described in the previous section indicates that the electron heat transport is transiently reduced in relation to the $\tilde{n}/n$ reduction. However, in this simulation, the time scale for the χ_e reduction (≥15 ms) is longer than the time scale for the $P_{refl.}^{H}$ reduction (<5 ms) and is similar to the time scale for the T_e change. The χ_e reduction seems to be coupled with the T_e change rather than the $\tilde{n}/n$ reduction. This result is consistent with the result of the power balance analysis, where χ_e after the $\tilde{n}/n$ reduction is almost the same as that before the $\tilde{n}/n$ reduction with the identical T_e profile fully relaxed/recovered from the transient phase, as shown in Fig. 2. It should be investigated whether the time scale for the χ_e reduction same as the time scale for the $\tilde{n}/n$ reduction can reproduce the transient T_e behavior or not in future work to understand the relation between the χ_e reduction and the $\tilde{n}/n$ reduction.

Acknowledgement

This work was partly supported by JSPS, Grant-in-Aid for Scientific Research (A) No. 16206093.

References

[1] E. Mazzucato et al., Phys. Rev. Lett. **77**, 3145 (1996).
[2] R. Nazikian et al., Phys. Rev. Lett. **94**, 135002 (2005).
[3] N. Oyama et al., Plasma Phys. Control. Fusion **46**, A355 (2004).
[4] H. Takenaga and the JT-60 team, Phys. Plasmas **8**, 2217 (2001).
[5] L. G. Bruskin et al., Plasma Phys. Control. Fusion **44**, 2305 (2002).
[6] H. Takenaga et al., Nucl. Fusion **43**, 1235 (2003).
[7] S. Inagaki et al., 20th IAEA Fusion Energy Conf. (Vilamoura, 2004) IAEA-CN-116/EX/P2-12; submitted to Nucl. Fusion.
[8] P. Mantica et al., Plasma Phys. Control. Fusion **44**, 2185 (2002).